REFERENCES

1. Mosmann T. Rapid colormetric assay for cellular growth and survival: application to proliferation and cytotoxity assays. *J Immunol Methods* 1983;65:55–63.
2. Kuzmits R, Aigiger P, Frass M, et al. Influence of cytostatics on ATP-levels of leukemic cells. *Adr Exp Med Biol* 1984;165:383–388.
3. Salmon SE, Alberts DS, Durie BGM, et al. Clinical correlations of drug sensitivity in the human stem cell assay: recent results. *Cancer Res* 1980;74:300–305.
4. Tanigawa N, Kern DH, Hikasa Y, Morton DL. Rapid assay for evaluating the chemosensitivity of human tumors in soft agar culture. *Cancer Res* 1982;42:2159–2164.
5. Weisenthal LM, Marden JA, Dill PL, Macaluso CK. A novel dye exclusion method for testing in vitro chemosensitivity of human tumors. *Cancer Res* 1983;43:749–757.
6. Hoffman RM, Connors KM, Meerson-Monosov AZ, Herrera H, Price JH. A general native-state method for determination of proliferation capacity of human normal and tumor tissues in vitro. *Proc Natl Acad Sci USA* 1989;86:2013–2017.
7. Povlsen CO, Jacobsen GK. Chemotherapy of a human malignant melanoma transplanted in the nude mouse. *Cancer Res* 1975;35:2790–2796.
8. Bogden AE, Haskell PM, Lepage DJ, Kelton DE, Cobb WR, Esber HJ. Growth of human xenografts implanted under the renal capsule of normal immunocompetent mice. *Exp Cell Biol* 1979;47:281–293.
9. Reivich M, Kuhl D, Wolf A, et al. The [^{18}F]fluorodeoxyglucose method for measurement of local cerebral glucose utilization in man. *Circ Res* 1979;44:127–137.
10. Gallagher BM, Flowler JS, Gutterson NI, MacGregor RR, Wan CN, Wolf AP. Metabolic trapping as a principle of radiopharmaceutical design: some factors responsible for the biodistribution of [^{18}F]2-deoxy-2-fluoro-D-glucose. *J Nucl Med* 1978;19:1154–1161.
11. Warburg O. On the origin of cancer cells. *Science* 1956;123:309–314.
12. Di-Chiro G. Positron emission tomography using [^{18}F]fluorodeoxyglucose in brain tumors. A powerful diagnostic and prognostic tool. *Invest Radiol* 1986;22:360–371.
13. Yonekura Y, Benua RS, Brill AB, et al. Increased accumulation of 2-deoxy-2-(F-18)F-fluoro-D-glucose in liver metastases from colon carcinoma. *J Nucl Med* 1982;23:1133–1137.
14. Abe Y, Matsuzawa T, Fujiwara T, et al. Clinical assessment of therapeutic effects on cancer using ^{18}F-2-fluoro-2-deoxy-D-glucose and positron emission tomography: preliminary study of lung cancer. *Int J Radiat Oncol Biol Phys* 1990;19:1005–1010.
15. Wahl RL, Zasadny K, Helvie M, et al. Metabolic monitoring of breast cancer chemohormonotherapy using positron emission tomography: initial evaluation. *J Clin Oncol* 1993;11:2101–2111.
16. Haberkorn U, Strauss LG, Dimitrakopoulou A, et al. Fluorodeoxyglucose imaging of advanced head and neck cancer after chemotherapy. *J Nucl Med* 1993;34:12–17.
17. Nagata Y, Yamamoto K, Hiraoka M, et al. Monitoring liver tumor therapy with [^{18}F]FDG positron emission tomography. *J Comput Assist Tomogr* 1990;14:370–374.
18. Bares R, Klever P, Hauptmann S, et al. F-18 fluorodeoxyglucose PET in vivo evaluation of pancreatic glucose metabolism for detection of pancreatic cancer. *Radiology* 1994;192:79–86.
19. Okada J, Yoshikawa K, Itami M, et al. Positron emission tomography using fluorine-18-fluorodeoxyglucose in malignant lymphoma: a comparison with proliferative activity. *J Nucl Med* 1992;33:325–329.
20. Higashi K, Clavo AC, Wahl RL. Does FDG uptake measure proliferative activity of human cancer cells? In vitro comparison with DNA flow cytometry and tritiated thymidine uptake. *J Nucl Med* 1993;34:414–419.
21. Takahashi H, Yamagichi K, Wakui A, et al. New approach to clinical evaluation of cancer chemotherapy using positron emission tomography with ^{18}F-FDG (2-deoxy-2-[^{18}F]fluoro-D-glucose). *Sci Res Inst Tohoku Univ* 1986;69:830–838.
22. Minn H, Paul R, Ahonen A. Evaluation of treatment response to radiation in head and neck cancer with fluorine-18 fluorodeoxyglucose. *J Nucl Med* 1988;29:1521–1525.
23. Minn H, Soini I. Fluorine-18-fluorodeoxyglucose scintigraphy in diagnosis and follow up of treatment in advanced breast cancer. *Eur J Nucl Med* 1989;15:61–66.
24. Ichiya Y, Kuwabara Y, Otsuka M, et al. Assessment of response to cancer therapy using fluorine-18-fluorodeoxyglucose and positron emission tomography. *J Nucl Med* 1991;32:1655–1660.
25. Abe Y, Matsuzawa T, Fujiwara T, et al. Assessment of radiotherapeutic effects on experimental tumors using ^{18}F-2-fluoro-2-deoxy-D-glucose. *Eur J Nucl Med* 1986;12:325–328.
26. Higashi K, Clavo AC, Wahl RL. In vivo assessment of 2-fluoro-2-deoxy-D-glucose, L-methionine and thymidine as agents to monitor the early response of a human adenocarcinoma cell line to radiotherapy. *J Nucl Med* 1993;34:773–779.
27. Shiue CY, Salvadori PA, Wolf AP, Fowler JS, MacGregor RR. A new improved synthesis of 2-deoxy-2-[^{18}F]fluoro-D-glucose from ^{18}F-labeled acetyl hypofluorite. *J Nucl Med* 1982;23:899–903.
28. Kondo T, Imaizumi M, Taguchi T, et al. A model for chemosensitivity determination of anticancer agents against human cancer using nude mice. *Jpn Cancer Chemother* 1987;14:680–686 (in Japanese).
29. Geran RI, Greenberg NH, Macdonald MM, Shumacher AM, Abbott BJ. Protocols for screening chemical agents and natural products against animal tumors and other biological systems. *Cancer Chemother Res* 1972;3:51–61.
30. Minn H, Joensuu H, Ahonen A, Klemi P. Fluorodeoxyglucose imaging: a method to assess the proliferative activity of human cancer in vivo. Comparison with DNA flow cytometry in head and neck tumors. *Cancer* 1988;61:1776–1781.
31. Yoshioka T, Takahashi H, Oikawa H, et al. Accumulation of 2-deoxy-2[^{18}F]fluoro-D-glucose in human cancer heterotransplanted in nude mice: comparison between histology and glycolytic status. *J Nucl Med* 1994;35:97–103.
32. Shimoyama Y, Kubota T, Inoue S, et al. Antitumor activity of cisplatin and carboplatin against human tumor xenografts serially transplanted into nude mice with reference to gastric carcinomas. *Jpn J Cancer Chemother* 1987;14:2682–2687.
33. Kikuchi H, Asamura M, Gamoh M, Matsushita T, Wakui A, Takahashi T. An experimental study on SRCA (subrenal capsule assay)–using some immunosuppressive maneuvers. *Jpn J Cancer Chemother* 1988;15:2257–2263.
34. Eder JP, Elias A, Shea TC, et al. A Phase I-II study of cyclophosphamide, thiotepa and carboplatin with autologous bone marrow transplantation in solid tumor patients. *J Clin Oncol* 1990;8:1239–1245.
35. Antman K, Ayash L, Elias A, et al. A Phase II study of high dose cyclophosphamide, thiopenta and carboplatin with autologous marrow support in women with measurable advanced breast cancer responding to standard-dose therapy. *J Clin Oncol* 1992;10:102–110.

Transcobalamin II Receptor Imaging via Radiolabeled Diethylene-Triaminepentaacetate Cobalamin Analogs

Douglas A. Collins and H.P.C. Hogenkamp

Department of Diagnostic Radiology, Mayo Clinic, Rochester; and Department of Biochemistry, University of Minnesota, Minneapolis, Minnesota

Rapidly dividing cells up-regulate the number of transcobalamin II receptors during DNA replication. We have developed diethylene-triaminepentaacetate (DTPA) cobalamin analogs for the purpose of imaging transcobalamin II receptors in malignant and nonmalignant tissue. **Methods:** Methyl-, adenosyl- and cyanocobalamin-b-(4-aminobutyl)-amide-DTPA analogs were synthesized. In vitro binding of the analogs to the transcobalamin proteins was assessed by the unsaturated vitamin B12 binding capacity assay and compared to DTPA and cyanocobalamin. The biodistribution of the ^{111}In-DTPA cobalamin analogs was measured at 24 hr after injection into sarcoma-bearing mice and non-tumor-bearing mice and pigs. **Results:** Methyl-, adenosyl- and cyanocobalamin-b-(4-aminobutyl)-amide-DTPA analogs and DTPA were 94.0%, 90.4%, 66.4%, and 3.6%, respectively, as efficient in binding to the transcobalamin proteins when compared to cyanocobalamin. At 24 hr after administration, the cobalamin analogs had 5–17 times and 20–29 times, respectively, the amount of uptake within the resected tissue samples and transplanted sarcomas when compared to ^{111}In-DTPA. **Conclusion:** The radiolabeled DTPA cobalamin analogs are biologically active. Preliminary animal studies suggest that the analogs could be effective in vivo transcobalamin II receptor imaging agents.

Key Words: receptor imaging; tumor-seeking agent; vitamin B12

J Nucl Med 1997; 38:717–723

Vitamin B12 (cyanocobalamin) has two coenzymatic functions in humans. Methylcobalamin serves as the cytoplasmic coenzyme for ^{5}N-methyltetrahydrofolate:homocysteine methyl transferase (methionine synthetase, EC 2.1.1.13), which cata-

Received Feb. 1, 1996; revision accepted Aug. 8, 1996.

For correspondence or reprints contact: Douglas A. Collins, MD, Mayo Clinic, 200 First Street SW, Rochester, MN 55905.

lyzes the formation of methionine from homocysteine. Adenosylcobalamin is the mitochondrial coenzyme for methylmalonyl-CoA mutase (EC 5.4.99.2), which interconverts methylmalonyl CoA and succinyl CoA. Transcobalamin II and intrinsic factor (IF) are the carrier proteins responsible for cobalamin transport within the intravascular/extracellular space and gastrointestinal tract, respectively. Cellular uptake of the cobalamins is regulated by cell membrane transcobalamin II receptors.

Rapidly proliferating cells have increased uptake of thymidine and methionine (*1–8*). Up-regulation in the number of transcobalamin II receptors has been demonstrated in several malignant cell lines during accelerated thymidine incorporation and DNA synthesis (*9–15*). Since methylcobalamin is directly involved with methionine synthesis, and therefore indirectly involved in the production of thymidylate and DNA; and because adenosylcobalamin is involved with mitochondrial metabolism, it is not surprising that radiolabeled vitamin B12 ([^{57}Co]cyanocobalamin) has increased uptake in rapidly dividing tissue (*16–20*).

Unfortunately, the long half-life of ^{57}Co (270.9 days) and the low specific activity of [^{57}Co]cyanocobalamin (16.5–37 kBq/μg) makes this vitamin B12 radiopharmaceutical unsuitable for clinical tumor imaging. However, vitamin B12 has several characteristics that potentially make it an attractive in vivo tumor-imaging agent. Vitamin B12 is water-soluble, has no known toxicity and, in excess, is excreted by glomerular filtration. These characteristics prompted us to re-examine the use of radiolabeled vitamin B12 as a tumor-imaging agent.

In this communication we will describe (*1*) methods for covalently attaching diethylene-triaminepentaacetate (DTPA) to methyl-, adenosyl- and cyanocobalamin; (*2*) the interaction of the DTPA cobalamin analogs (DCAs) with the transcobalamin proteins (TPs) and IF; and (*3*) preliminary swine and murine biodistribution data.

MATERIALS AND METHODS

Synthesis of DCAs

Cyanocobalamin and 1-ethyl-3(3-dimethylaminopropyl) carbodiimide were purchased from Sigma (St. Louis, MO). Adenosine, 1,4-diaminobutane dihydrochloride, DTPA, hexamethylphosphoramide, 1-hydroxybenzotriazole hydrate, iodomethane and thionylchloride were purchased from Aldrich (St. Louis, MO). Thin-layer chromatography (TLC) silica gel and PET-cellulose sheets were purchased from E.M. Science (Gibbstown, NJ). Other inorganic salts and solvents were obtained in the highest purity available. Ultraviolet-visible spectra were recorded on a diode array spectrophotometer. DTPA dianhydride and 5′-chloro-5′-deoxyadenosine were synthesized as described by Eckelman et al. (*21*) and Kikugawa and Ichino (*22*), respectively. The b-monocarboxylic acids of methyl-, adenosyl- and cyanocobalamin were prepared as previously described (*23–26*).

Reaction mixtures containing the methyl-, adenosyl- and cyanocobalamin-b-monocarboxylic acids (1.0 g, 0.6 mmol) hydroxybenzotriazole (0.81 g, 6 mmol) and 1,4-diaminobutane dihydrochloride (4.8 g, 30 mmol) in 100 ml of water were adjusted to pH 7.8 with sodium hydroxide. 1-Ethyl-3(3′-dimethyl aminopropyl) carbodiimide (1.26 g, 6.6 mmol) was then added, the pH was adjusted to 6.4 and the reaction was stirred at room temperature for 24 hr. TLC on silica gel using n-butanol/acetic acid/water (5:2:3) showed the reaction to be complete. The 4-amino-butyl amides were extracted into 92% aqueous phenol, and the phenol phase was washed exhaustively with water to remove the other reactants. One volume of acetone and three volumes of ether were added to the phenol phase. The desired cobalamins were removed from the organic solvents by several extractions with water. The combined aqueous layers were extracted three times with ether to remove residual phenol, concentrated to ~20 ml in vacuo and finally crystallized from aqueous acetone.

The cobalamin-b-(4-aminobutyl) amides (500 mg, 0.3 mmol) were then separately dissolved in 30 ml of saturated sodium bicarbonate and treated with a 10-fold excess (1.2 g, 3.4 mmol) of solid DTPA dianhydride. The progress of the reaction was monitored by TLC on PEI plates using n-butanol-acetic acid-water (5:2:3) as the solvent. After 30 min of incubation at room temperature, a second 1.2 g of dianhydride was added. The pH was then adjusted to 8.2 and the reaction mixture was incubated overnight. The DCAs were then extracted into 92% aqueous phenol and purified as described above. The preparations resisted crystallization from aqueous acetone; therefore the analogs were evaporated to dryness and isolated as glasses.

In Vitro Biological Activity of DCAs

To assess the in vitro binding of DCAs to the TPs and IF, the unsaturated vitamin B12 binding capacity (UBBC) and the IF blocking antibody (IFBA) assays were performed. Serum was obtained from five patients being evaluated for pernicious anemia at the Mayo Clinic. The patients' serum first underwent routine clinical UBBC and IFBA assays as previously described (*27–30*). To determine if DCAs would inhibit [^{57}Co]cyanocobalamin from binding to TP and IF, the excess serum from the five patients underwent modified UBBC and IFBA assays.

Specifically, under dim light, 1 mg of the nonlabeled methylcobalamin-b-(4-aminobutyl)-amide DTPA (DTPA-MEB12), adenosylcobalamin-b-(4-aminobutyl)-amide DTPA (DTPA-ADB12) and cyanocobalamin-b-(4-aminobutyl) amide-DTPA (DTPA-CNB12), as well as 1 mg each of cyanocobalamin and DTPA, were separately dissolved in 10 ml of normal saline at room temperature. To potentially saturate all TP- and IF-binding sites, 1-μl aliquots of the five solutions were separately incubated with the serum from each patient as well as with purified IF for 20 min at room temperature and for another 20 min at 4°C. The presaturated serum and purified IF then underwent routine clinical UBBC and IFBA protocols.

Radiolabeling of DCAs

Before in vivo studies, an approximation of the specificity activity of DCAs was assessed via TLC, radiochromatography (RC) and gamma well counting. The TLC strips (grade 31 ET Chr; thickness, 0.50 mm; flow rate (water), 225 mm/30 min) were developed with acetone in dim light. The dried strips were placed on film for 1–5 min before development. TLC and RC results were visually compared. The upper 25% and lower 75% of the TLC strips were separately counted for 5 min in a gamma well counter at 18 hr after acetone development.

Approximation of the specific activity of ^{99m}Tc-labeled DCAs was assessed by mixing 100-μl aliquots of DTPA-MEB12 and DTPA-ADB12 (5 μg/100 μl of normal saline) with 50 μl of stannous chloride solution (5 μg/50 μl of normal saline) in nitrogen-purged 2-ml vials. Increasing increments (370 MBq) of ^{99m}Tc were then titrated into the sealed vials. After the addition of ^{99m}Tc, the solutions were mixed gently and purged with nitrogen for 5 min. For comparison, the analogs underwent ^{99m}Tc labeling in room air in the absence of stannous chloride. A control solution of cyanocobalamin (5 μg/100 μl of normal saline) was mixed with ^{99m}Tc at room temperature in room air, as well as within nitrogen purged 2 ml vials containing 50 μl of the stannous chloride solution. The specific activity for indium-labeled DCAs was assessed in a similar manner. Increasing amounts (3.7 MBq) of ^{111}In-chloride was titrated into 2-ml vials containing 100 μl (1 μg

TABLE I
Transcobalamin and IF Binding

	CNB12 (%)	DTPA-MEB12 (%)	DTPA-ADB12 (%)	DTPA-CNB12 (%)	DPTA (%)
UBBC	100	94.0	90.4	66.4	3.6
IFBA	92.5	63.2	41.0	52.9	0.8

CNB12 = cyanocobalamin (vitamin B12).

of DCA/100 μl of saline) of DTPA-MEB12 or DTPA-ADB12. All ^{111}In mixtures were incubated for 10 min at room temperature in room air. Cyanocobalamin underwent identical ^{111}In labeling and analysis.

To ensure complete binding of the radionuclides for the in vivo studies, excess chelator in a ratio of 40–200 μg of DCA or DTPA to 37.0 MBq of ^{99m}Tc or ^{111}In was used during labeling. TLC and RC analyses were performed to confirm 100% labeling before in vivo administration.

Murine Biodistribution Studies

Groups of three 12-wk-old female Balb-c mice were injected i.p. with 18.5 MBq of either DTPA-ADB12 or DTPA (111 MBq of ^{111}In/300 μg of DCA or DTPA/1 ml of normal saline) and killed at 24 hr. Several mice were injected i.v. with ~200 μl of DTPA-MEB12 (185 MBq of ^{99m}Tc/1 mg of DCA/1 ml of normal saline) and killed at varying time intervals after injection. All mice were placed in sterile containers after i.p. or i.v. administration, and the first passed urine was collected and analyzed via TLC and RC.

DTPA-MEB12 and DTPA (111 MBq of ^{111}In/300 μg of DCA or DTPA/100 μl of normal saline) were used to assess biodistribution after oral administration. Two drops of either ^{111}In-DTPA or ^{111}In-DTPA-MEB12 were placed in the oral cavities of two groups of three mice. A "modified Schilling test" was performed on two mice. Specifically, each mouse received s.c. and i.p. administration a 1-mg loading dose of nonlabeled DTPA-MEB12. After 24 hr, the mice were fed 2–3 drops of ^{111}In-DTPA-MEB12. All mice receiving radiolabeled compounds orally had their urine and feces collected for 8 hr and analyzed by gamma well counting. All mice were killed at 24 hr after ingestion of tracer.

Tumor Imaging

A sarcoma cell line, ATCC CCL8 (*8*), was grown in a monolayer in 10% Eagle's cell culture medium at 37°C and 8% CO_2. The cells were harvested by trypsinization, washed and collected in phosphate-buffered saline. The washed tumor cells (1×10^6 cells) were then sterilely injected subcutaneously into the left flank of female Balb-c mice. A 5- to 7-mm tumor developed in the left flank of the mice 5 days after innoculation.

Five days after tumor innoculation, two groups of three mice received either 200 μl (18.5 MBq) of ^{111}In-DTPA-ADB12 or DTPA (111 MBq of ^{111}In/300 μg of DCA or DTPA/1 ml of normal saline) via i.p. injection. Another two groups of three mice received ~3.7 MBq of the radiolabeled DCA or DTPA by tail vein injection. The tumor-bearing mice were killed at 24 hr after DCA or DTPA administration.

All mice were killed via CO_2 inhalation before imaging or dissection. The pancreas, spleen, kidneys and heart were resected en bloc. A portion of the liver, lungs, left quadriceps muscle and flank fat were also harvested. All tissue samples and organs were weighed wet, minced in 2 ml of normal saline and counted for 5 min in a gamma well counter.

All images for the murine in vivo studies were obtained on a maxicamera using a LEAP collimator with a 20% window about the 140-keV energy peak of ^{99m}Tc and a medium-energy collimator with a 20% window about the 174-keV and 247-keV energy peaks of ^{111}In. A 256 × 256 matrix with a dedicated Pinnacle computer system was used to collect and analyze the data.

Swine Biodistribution

Two 35-lb female white domestic pigs were injected via an ear vein with ^{111}In-DTPA-ADB12 (277.5 MBq of ^{111}In/300 μg of DCA/10 ml of normal saline). For comparison, one 35-lb pig was injected i.v. with ^{111}In-DTPA (277.5 MBq of ^{111}In/300 μg of DTPA/10 ml of normal saline).

Biodistribution data was collected in a similar manner, except that only a small portion of each organ and tissue was sampled. The pigs were killed before imaging or dissection by i.v. administration of Sleepaway. Images were obtained on a whole-body camera using medium-energy collimators with a 20% window about the 174-keV and 247-keV energy peaks of ^{111}In and a scan speed of 5 cm/min.

RESULTS

Synthetic Yield

The methyl-, adenosyl- and cyanocobalamin-b-(4-aminobutyl)-amides were produced in yields of 920 mg (88%), 366 mg (77%) and 955 mg (92%), respectively. The yields of the methyl-, adenosyl- and cyanocobalamin amide-DTPA analogs were 600 mg (96%), 400 mg (80%) and 460 mg (77%), respectively.

Characterization of DCAs

The ultraviolet-visible spectra of the three DCAs are typical of their parent cobalamins. The DCAs are readily separated from their respective precursors by TLC on polyethylene imino (PEI) plates. The negatively charged complexes bind strongly at the origin in contrast to the precursors.

Interaction with the TPs and IF

Nonlabeled DCAs competitively blocked [^{57}Co]cyanocobalamin from binding to TP and IF. Therefore, the cpm of the modified UBBC and IFBA assays were significantly lower than that of the clinical runs. The percent binding (PB) of DCAs to TP or IF was calculated as follows: $PB = 100 - (DCA_{UBBC\ or}$

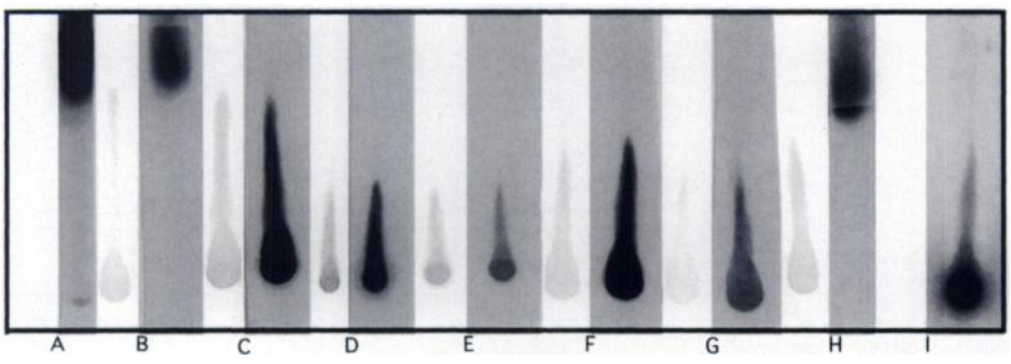

FIGURE 1. TLC with corresponding RC. (A) Free ^{99m}Tc. (B) Cyanocobalamin + ^{99m}Tc + SnCl + N_2. (C) DTPA-CNB12 + ^{99m}Tc + SnCl + N_2. (D) DTPA-MEB12 + ^{111}In. (E) DTPA-ADB12 + ^{111}In. (F) ^{99m}Tc-DTPA-MEB12 from urine after i.v. injection. (G) ^{99m}Tc-DTPA-ADB12 from urine after i.p. injection. (H) DTPA-MEB12 + ^{99m}Tc + room air. (I) 370 MBq ^{99m}Tc/μg DTPA-ADB12 + SnCl + N_2.

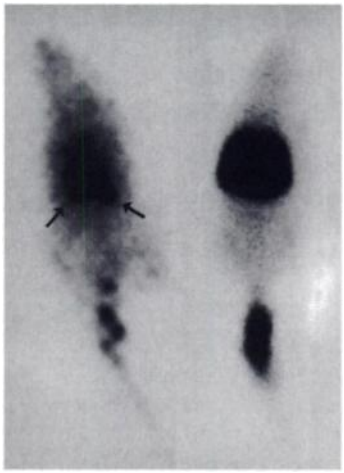

FIGURE 2. Biodistribution of DTPA-MEB12 at 5 min (left) and 4 hr (right) after tail vein injection. On the left, arrows indicate early renal uptake.

$_{IFBA}$ cpm/clinical$_{UBBC\ or\ IFBA}$ cpm × 100). The average percent binding of the five solutions (n = 10 for each solution—i.e., two modified UBBC and IFBA assays per patient) is shown in Table 1.

Approximation of Specific Activity

The methyl- and adenosylcobalamin-b-(4-aminobutyl) amide-DTPA analogs consistently bound 1.8 GBq of ^{99m}Tc/5 μg of DCA; and 40.5 MBq of ^{111}In/1 μg of DCA with 99.9% efficiency (n = 7). Radioactivity on the lower 75% of the TLC strips would overwhelm the gamma well counter immediately after development. Therefore counting of the divided TLC strips was performed at 18 hr after acetone development. As expected, there was minimal labeling of DCAs with ^{99m}Tc when stannous chloride and hypoxic conditions were not used. The two radionuclides did not bind to cyanocobalamin (Fig. 1).

Murine Biodistribution

No ill effects or deaths were observed after i.p., i.v., s.c. or PO administration of DCAs. The first passed urine after i.v. or i.p. injection was always radioactive. Because of the larger volume administered, the first passed urine was red in color, whereas it was usually pink after i.v. administration. TLC and RC analyses of the collected urine demonstrated 100% binding of ^{99m}Tc and ^{111}In to DCAs. (Fig. 1). Images at 5 min and 4 hr after tail vein injection showed prominent early uptake within the kidneys, which became obscured by the liver, spleen and gastrointestinal activity on the delayed images (Fig. 2). At 24 hr, the greatest amount of uptake was in the kidneys, followed by the liver and spleen. The pancreas usually was next followed by the lungs, fat, heart and muscle (Fig. 3).

The greatest amount of ^{111}In-DTPA uptake was in the kidneys. The distribution of DTPA was similar to DCAs. However, ^{111}In-DTPA had 5–12 times less activity per tissue sample when compared to the methyl- and adenosylcobalamin analogs.

Indium-111-DTPA-MEB12 was absorbed from the gastrointestinal tract after oral administration. The mice that underwent the modified Schilling test had detectable radioactivity within their urine by 1 hr. Images of these "flushed" mice at 24 hr demonstrated significantly less activity throughout the body when compared to the "nonflushed" mice (Fig. 4). No measurable activity was detected in the urine by gamma well counting in the mice that were not flushed with s.c. and i.p. doses of the nonlabeled DTPA-MEB12. At 2 hr after injection, ^{111}In DTPA was detected in urine. However, the activity was ~1% that of the ^{111}In DTPA-MEB12. Fecal radioactivity became detectable at 2 hr in all groups ingesting radiolabeled DTPA-MEB12 and DTPA.

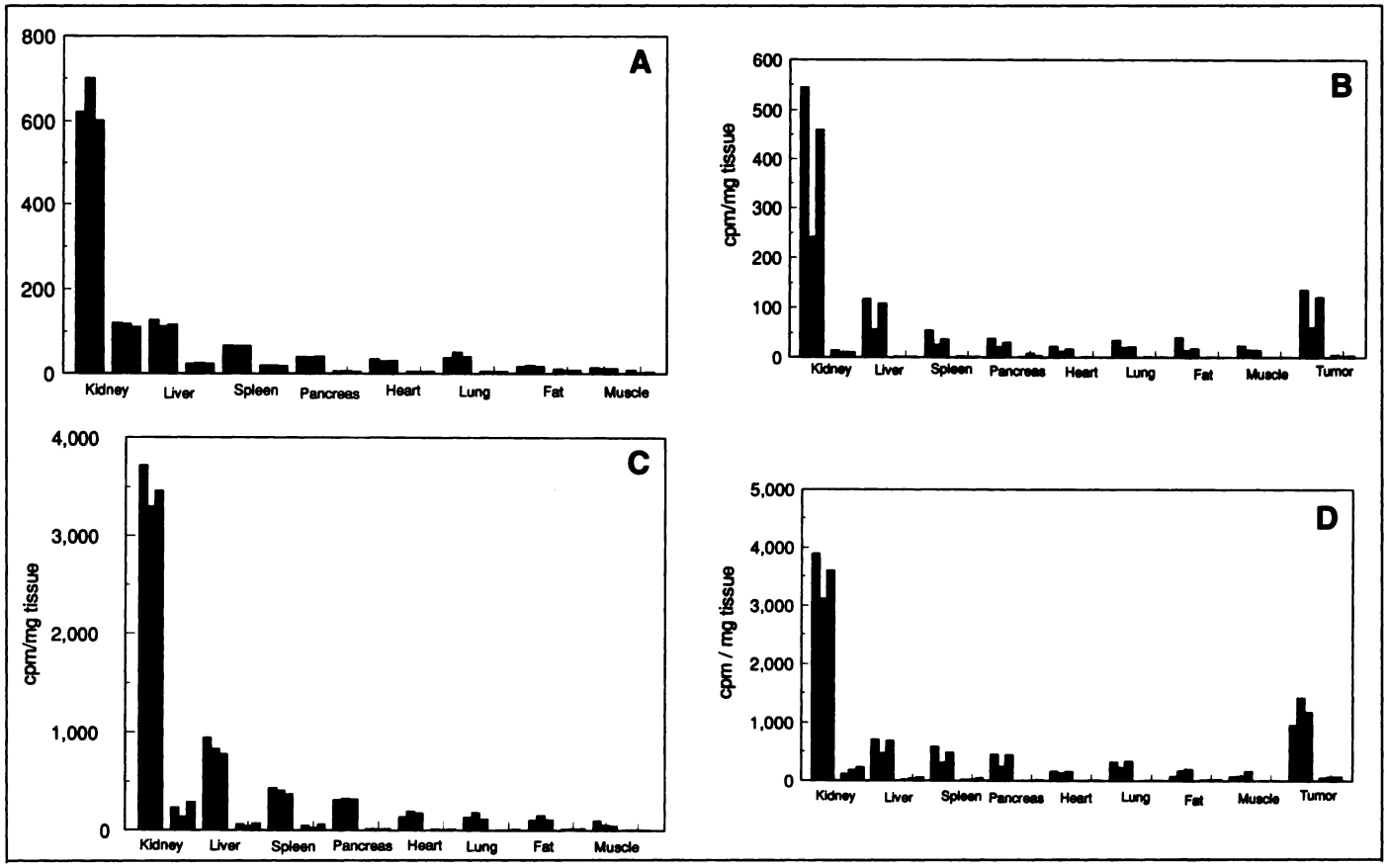

FIGURE 3. Each bar represents a single mouse. The top two (A, B) and bottom two (C, D) bar graphs depict biodistribution after i.v. and i.p. administration, respectively. Cross-hatched bars = DTPA-ADB12. Solid black bars = DTPA.

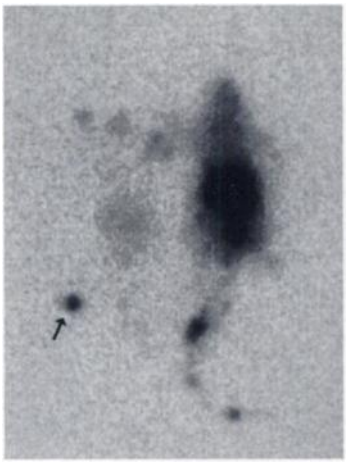

FIGURE 4. Ventral views with mice oriented nose up. The flushed mouse is on the left and has a contaminated right foot pad (arrow). The mice were simultaneously imaged for 12 hr.

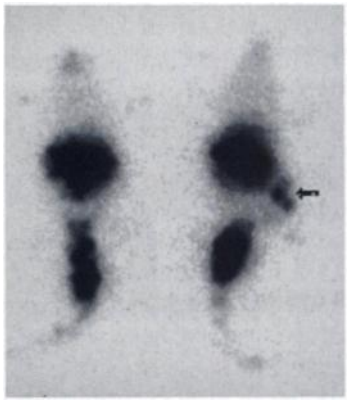

FIGURE 5. Ventral views with mice oriented nose up. Tumor bearing mouse on the right. Arrow indicates uptake within the transplanted sarcoma after tail vein injection. Image acquisition time was 10 min.

Tumor Imaging

At 24 hr, DCA uptake within the transplanted sarcomas was 2–4 times greater than that within the liver, spleen and pancreas, and 5–12 times greater than that in the heart, lungs, fat and muscle (Figs. 3 and 5). Gross pathology of the dissected masses demonstrated fat-encapsulated tumors. Microscopically, no areas of necrosis were identified. By hematoxylin and eosin staining, the tumors were solid masses of blue cells consistent with sarcomatous tissue.

Although ^{111}In-DTPA demonstrated uptake within the transplanted tumors, its concentration was 20–29 times less than that of ^{111}In-DTPA-ADB12.

Swine Biodistribution

No apparent side effects were noted after i.v. administration of the cobalamin analogs. The porcine biodistribution of DCAs was almost identical to that seen in the mice. Once again, DTPA had a similar biodistribution to the cobalamin analogs, but had 5–17 times less activity (except for the kidneys) per organ and/or tissue sample. DCA activity within the extremities may be in the bone marrow or epiphyseal growth plates. This finding was not directly investigated. The small bowel and colon had significant uptake, both visually and by gamma well counting (Fig. 6).

DISCUSSION

The synthesis of the three DCAs involves just two reactions starting from the cobalamin-b-monocarboxylic acids. In the first reaction, an aminobutyl group was coupled to the monocarboxylic acids. The resulting methyl-, adenosyl- and cyanocobalamin-b-(4-aminobutyl) amides were isolated as homogenous crystalline preparations. In the second reaction, DTPA was attached to the cobalamin-amides to generate the desired methyl-, adenosyl- and cyanocobalamin-b-(4-aminobutyl)-amide-DTPA complexes.

Since both methylcobalamin and adenosylcobalamin are light-sensitive, all manipulations involving these two corrinoids were performed in the dark or in dim light. In addition, the carbon–cobalt bond of adenosylcobalamin undergoes heterolytic change in the presence of cyanide ion. Thus, cyanide salts were not included in the UBBC and IFBA assays.

For cobalamin to be a useful imaging agent, any modification of it should not significantly inhibit its interaction with the carrier proteins transcobalamin II and IF. A simple alteration of the UBBC and IFBA clinical assays allows for an in vitro approximation of these interactions. Table 1 demonstrates that the cobalamin–DTPA complexes are biologically active. However, the attachment of DTPA to the cobalamins does affect their binding to the carrier proteins, especially to IF.

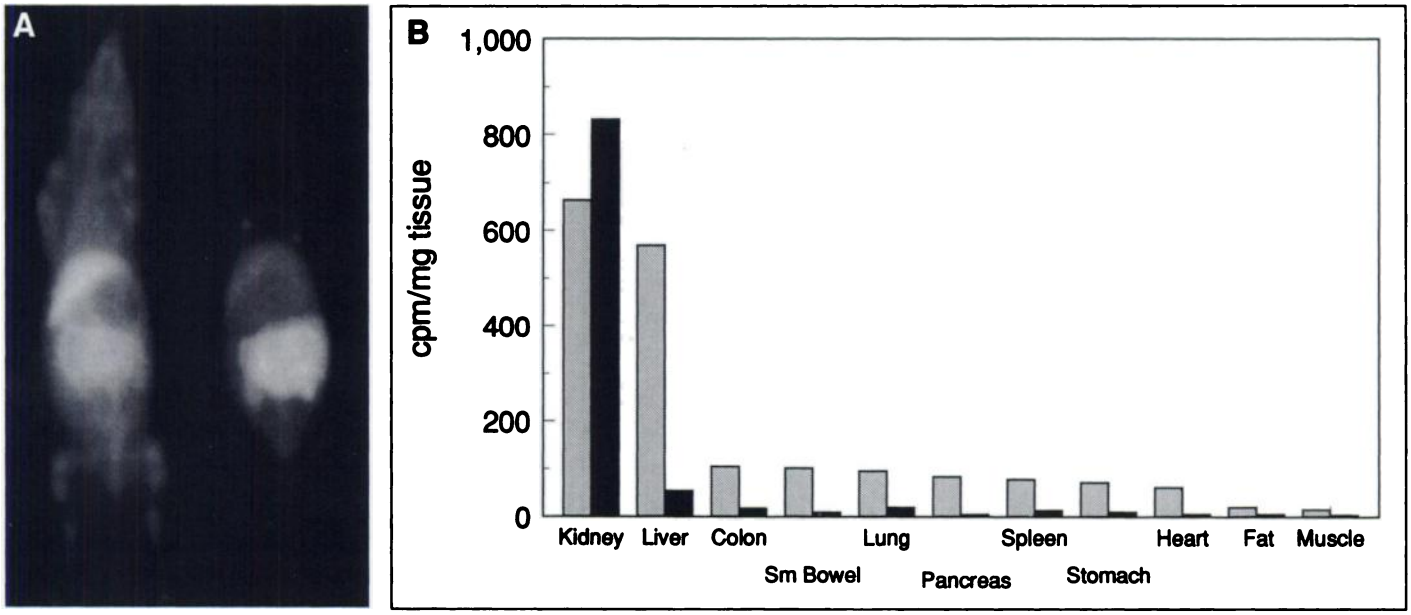

FIGURE 6. The ventral view of the pigs is oriented snout up. (A) The pigs on the left and right demonstrate biodistribution of ^{111}In-ADB12 and ^{111}In-DTPA, respectively. (B) Cross-hatched bar = DTPA-ADB12 (n = 2). Solid black bar = DTPA (n = 1).

The decreased affinity of IFs for the DCAs compared to the TPs is consistent with prior studies. Rosenblum et al. (*31–33*) found that modifications of the six substituent and the benzimidazole group of vitamin B12 had little effect on the biodistribution of the analogs after i.v. administration (transcobalamin II binding). However, the analogs were half as likely to be absorbed after oral administration when compared to [^{60}Co]cyanocobalamin (IF binding).

Since Mayo Medical Laboratory does not separate the UBBC assay into transcobalamin II and transcobalamin I/III fractions, the interaction of the analogs with transcobalamin II could not be directly studied. Therefore, a modified Schilling test was performed to indirectly demonstrate that nonlabeled DCAs could saturate in vivo transcobalamin II receptor sites. The overall biodistribution of DCAs is almost identical to previous studies performed with ^{60}Co- and ^{57}Co-radiolabeled vitamin B12, as well as with whole-body vitamin B12 microbiological assays (*34–38*). Figures 3 and 6 demonstrate that there are significant differences in the degree of organ and tumor uptake between DCAs and DTPA. These findings strongly suggest that DCA binds to transcobalamin II receptors in vivo. Since a large amount of nonlabeled DCAs was administered per biodistribution study (39–199 μg of nonlabeled DCA to 1 μg of radiolabeled DCA), the maximal cpm/mg of tissue or percent injected dose cannot be accurately determined.

In spite of the suboptimal labeling of DCAs, there was a significant amount of analog uptake within the tumors at 24 hr. The mice were killed at 24 hr for two reasons. First, prior studies have demonstrated that the maximal uptake of radiolabeled vitamin B12 occurs within tumors at 24 hr after i.v. or i.p. administration (*36–38*). Second, imaging at 5 days after inoculation and at 24 hr after tracer injection decreases the likelihood that the tracer is localizing within the tumors due to necrosis or hypervascularity.

The 12-wk-old female Balb-c mice did not demonstrate any ill effects from the cobalamin–DTPA complexes, despite receiving the usual loading dose (1 mg) of vitamin B12 for humans. This observation suggests that the DCAs are nontoxic. However, more extensive toxicology studies are needed.

Finally, the biodistribution of DTPA in our investigation is consistent with two prior studies. McAfee et al. (*39*) found that 4% of an i.v. administered dose of ^{111}In-DTPA remained unexcreted in dogs at 24 hr. The kidneys had the greatest amount of activity followed by the liver, small and large bowels, muscle, stomach and spleen. This observation was thought to be due to nonspecific binding of DTPA to proteins throughout the body. Stevens et al. (*40*) demonstrated in humans that a small amount of [^{14}C]DTPA was absorbed from the gastrointestinal tract after oral administration.

CONCLUSION

The reported results demonstrate that the attachment of DTPA to the vitamin B12 coenzymes, methyl- and adenosylcobalamin, does not greatly affect their interaction with the TPs. However, it does affect their interaction with IF. Under suboptimal labeling conditions, the specific activity of the ^{99m}Tc- and ^{111}In-DCAs is approximately 10,000 and 1100 times greater, respectively, than that of the clinically available vitamin B12 analog, [^{57}Co]cyanocobalamin. This should allow for in vivo imaging of transcobalamin II and possibly IF receptors. Transcobalamin II receptor-based tumor imaging may be feasible with these new cobalamin analogs.

ACKNOWLEDGMENTS

The authors express their appreciation to Rose Busta for the preparation of the manuscript and to Gina Scheidt and Kathy Kubik for performing the UBBC and IFBA assays. This study was supported by a grant from the Mayo Foundation (A-106-Z-94). H.P.C.H. was supported by the University of Minnesota.

REFERENCES

1. Ishiwata K, Takahashi T, Iwata R, et al. Tumor diagnosis by PET: potential of seven tracers examined in five experimental tumors including an artificial metastasis model. *Nucl Med Biol* 1992;19:611–618.
2. Schmall B, Conti PS, Schaeffer DJ, Kleinert EL. Tumor and organ biochemical profiles determined in vivo following uptake of a combination of radiolabeled substates: potential applications for PET. *Am J Physiol Imaging* 1992;7:2–11.
3. Kubota K, Ishiwata K, Kubota R, Yamada S, Tada M, Sato T, Ido T. Tracer feasibility for monitoring tumor radiotherapy: a quadruple tracer study with fluorine-18-fluorodeoxyglucose or fluorine-18-fluorodeoxyuridine, L-[methyl-14C] methionine, [6–3H]thymidine, and gallium-67. *J Nucl Med* 1991;32:2118–2123.
4. Shields AF, Lim K, Grierson J, Link J, Krohn KA. Utilization of labeled thymidine in DNA synthesis: studies for PET. *J Nucl Med* 1990;31:337–342.
5. Higashi K, Clavo AC, Wahl RL. In vitro assessment of 2-fluoro-2-deoxy-D-glucose, L-methione and thymidine as agents to monitor the early response of a human adenocarcinoma cell line to radiotherapy. *J Nucl Med* 1993;34:773–779.
6. Sato K, Kameyama M, Ishiwata K, Katakura R, Yoshimoto T. Metabolic changes of glioma following chemotherapy: an experimental study using four PET tracers. *J Neurooncol* 1992;14:81–89.
7. Kubota R, Kubota K, Yamada S, et al. Methionine uptake by tumor tissue. A microautoradiographic comparison with FDG. *J Nucl Med* 1995;36:484–492.
8. Goethals P, van Eijkeren M, Lodewyck W, Dams R. Measurement of [methyl-carbon-11] thymidine and its metabolites in head and neck tumors. *J Nucl Med* 1995;36:880–882.
9. Ryel EM, Meyer LM, Gams RA. Uptake and subcellular distribution of Vitamin B_{12} in mouse L1210 leukemic lymphoblasts. *Blood* 1974;44:427–432.
10. Hall CA, Colligan PD. The function of cellular transcobalamin II in cultured human cells. *Exp Cell Res* 1989;183:159–167.
11. Gimsing P, Hippe E. Cobalamin-dependent metabolism in chronic myelogenous leukemia determined by deoxyuridine suppression test and the formiminoglutamic acid and methylmalonate excretion in urine. *Am J Hematol* 1995;49:121–130.
12. Begley JA, Colligan PD, Chu RC. Synthesis and secretion of transcobalamin II by cultured astrocytes derived from human brain tissue. *J Neurol Sci* 1994;122:57–60.
13. Lindemans J, Kroes ACM, van Geel J, van Kapel J, Schoester M, Abels J. Uptake of transcobalamin II-bound cobalamin by HL-60 cells: effects of differentiation induction. *Exp Cell Res* 1989;184:449–460.
14. Amagasaki T, Green R, Jacobsen DW. Expression of transcobalamin II receptors by human leukemia K562 and HL-60 cells. *Blood* 1990;76:1380–1386.
15. Hall CA, Green-Colligan PD, Begley JA. The metabolism of cobalamin bound to transcobalamin II and to glycoproteins that bind Cbl in HepG2 cells (human hepatoma). *J Cell Physiol* 1985;124:507–515.
16. Cooper BA, Paranchyma W. Selective uptake of specifically bound cobalt-58 vitamin B_{12} by human and mouse tumor cells. *Nature* 1961;191:393–395.
17. Flodh H. Accumulation of labelled vitamin B-12 in some transplanted tumors. *Acta Radiol Suppl* 1968;284:55–60.
18. Blomquist L, Flodh H, Ullberg S. Uptake of labelled vitamin B-12 and 4-iosophenyl alanine in some tumours of mice. *Experientia* 1969;25:294–296.
19. Cooperman JM. Distribution of radioactive and nonradioactive vitamin B-12 in normal and malignant tissues of an infant with neuroblastoma. *Cancer Res* 1972;32:167–172.
20. Babior BM. *Cobalamin: biochemistry and pathophysiology*. New York: Wiley & Sons; 1975:289–333.
21. Eckelman WC, Karesh SM, Reba RC. New compounds: fatty acid and long chain hydrocarbon derivatives containing a strong chelating agent. *J Pharm Sci* 1975;64: 704–706.
22. Kikugawa K, Ichino M. *Tetrahedron Lett* 1971:87–90.
23. Hogenkamp HPC. Chemical synthesis and properties of analog of adenosylcobalamin. *Biochemistry* 1974;13:2736–2740.
24. Anton DL, Hogenkamp HPC, Walker TE, Matwivoff NA. Carbon-13 nuclear magnetic studies of the monocarboxylic acids of cyanocobalamin. Assignments of the b-, d-, and e-monocarboxylic acids. *J Am Chem Soc* 1980;102:2215–2219.
25. Yamada RH, Hogenkamp HPC. The synthesis of a 5′-deoxyadenosylcobalamin-agarose adsorbent and its utility in the purification of ribonucleotide reductase. *J Biol Chem* 1972;247:6266–6270.
26. Dolphin D. Preparation of the reduced forms of vitamin B_{12} coenzyme containing a cobalt–carbon bond. *Methods Enzymol* 1971:18;34–52.
27. Fairbanks VF, Lennon VA, Kokmen E, Howard FM. Tests for pernicious anemia: serum intrinsic factor blocking antibody. *Mayo Clin Proc* 1983;58:203–204.
28. Diagnostic Products Corporation. Product Insert. Intrinsic Factor Blocking Antibody [^{57}Co] Radioassay.
29. Grossowicz D, Sulitzeanu D, Merzbach D. Isotopic determination of vitamin B_{12} binding capacity and concentration. *Proc Soc Exp Biol Med* 1962;109:604–608.
30. Gottlieb C, Lau K-S, Wasserman LR, Herbert V. Rapid charcoal assay for intrinsic factor (IF), gastric juice unsaturated B_{12} binding capacity, antibody to IF, and serum unsaturated B_{12} binding capacity. *Blood* 1965;25:875–884.
31. Rosenblum C, RL Davis, BF Chow. Comparative absorption of vitamin B_{12} analogues by normal humans. III. 5,6-Dichlorobenzimidazole, 5,6-Desdimethylbenzimidazole and 5-Hydroxybenzimidazole analogues. *Proc Soc Exp Biol Med* 1957;95:30–32.
32. Rosenblum C, Woodbury DT, Gilbert JP, Okuda K, Chow BF. Comparative absorption of vitamin B_{12} analogues by normal humans. I. Chlorocobalamin vs. cyanocobalamin. *Proc Soc Exp Biol Med* 1955;89:63–65.

33. Rosenblum C, Yamamato RS, Wood R, Woodbury DT, Okuda K, Chow BF. Comparative absorption of vitamin B_{12} analogues by normal humans. II. Chloro-, sulfato-, nitro-, and thiocyanoto- vs. cyanocobalamin. *Proc Soc Exp Biol Med* 1956;91:364–366.
34. Cooperman JM, Luhby AL, Teller DN, Marley JF. Distribution of radioactive and nonradioactive vitamin B_{12} in the dog. *J Biol Chem* 1960;235:191–194.
35. Rappazzo ME, Salmi HA, Hall CA. The content of Vitamin B_{12} in adult and foetal tissue: a comparative study. *Br J Haematol* 1970;18:425–433.
36. Rigby CC, Bodian M. Experimental study of the relationship between vitamin B_{12} and two animal tumour systems. *Br J Cancer* 1963;17:90–99.
37. Warnock SH, Collins DA, Morton KA. Comparison of tumor uptake and nuclear medicine images of gallium-67, thallium-201, and cobalt-57–vitamin B-12 in sarcoma-bearing mice. *Clin Res* 1992;40:7A.
38. Wooley KE, Collins DA, Morton KA. Uptake of Co-57–vitamin B-12 by murine tumors of many histologic types. *Clin Res* 1993;41:73.
39. McAfee JG, Gagne G, Atkins HL, et al. Biological distribution and excretion of DTPA labeled with Tc-99m and In-111. *J Nucl Med* 1979;20:1273–1278.
40. Stevens E, Rosoff B, Weiner M, Spencer H. Metabolism of the chelating agent diethylenetriamine pentaacetic acid (^{14}CDTPA) in man. *Proc Soc Exp Biol Med* 1962;111:235–238.

Radioassay of Yttrium-90 Radiation Using the Radionuclide Dose Calibrator

Qansy A. Salako and Sally J. DeNardo
Molecular Cancer Institute, Department of Internal Medicine, University of California, Davis, Sacramento, California

Yttrium-90 is used in radioimmunotherapy because of its favorable physical half-life and energetic pure beta emissions. However, it is often necessary to standardize ^{90}Y sources to establish a dose calibrator dial setting for accurate calibration of clinical doses of ^{90}Y preparations. **Methods:** A solution of $^{90}YCl_3$ containing 2.81 kBq/ml (by supplier's calibration) was prepared by serial dilution in 0.05 *M* HCl. Ten 100-μl aliquots of this solution were counted in a Packard liquid scintillation analyzer; the mean radioactivity in becquerels was determined and used to evaluate dial settings 48 × 10, 775 × 70 and 775 × 100 on a radionuclide dose calibrator for ^{90}Y measurements. The dose calibrator response was also studied on ^{90}Y sources at varying solution volumes in plastic and glass containers. **Results:** Calibrator readings of ^{90}Y sources in glass and plastic vials and plastic syringes were accurate at either dial setting 48 × 10 (commonly used by many ^{90}Y laboratories) or 775 × 70. Measurements of 1.15 and 3.03 GBq (31 and 82 mCi, respectively) calibrated ^{90}Y sources in either vial were −3.0 and +4.3%, respectively, at dial-setting 775 × 70 and −4.0 and +9.0% at 48 × 10. Yttrium-90 sources in plastic syringes gave higher readings than those in glass vials, therefore, requiring a container correction factor for accurate dose assay. Measurements of $^{90}YCl_3$ shipments from four suppliers over a 3-yr period demonstrated concurring calibration measurements at both 775 × 70 and 48 × 10 settings for shipments from all suppliers. The dose calibrator response to ^{90}Y radiation was linear within a 1–333 kBq range in a constant sample volume of 580 μl. **Conclusion:** This work demonstrates the validity of using the 48 × 10 dial-factor combination on the standard radionuclide dose calibrator for calibration of ^{90}Y radiopharmaceuticals.

Key Words: yttrium-90; dose calibrator; assay; liquid scintillation; linearity test

J Nucl Med 1997; 38:723–726

Yttrium-90 has attracted much research attention in radioimmunotherapy because its 64-hr half-life and pure beta emissions are potentially useful for cancer therapy. Some of its unique advantages (*1–5*) include: availability of methods for attaching the radiometal to chelate-carrying proteins and antibodies; physical $T_{1/2}$ suited for tumor localization; long-range beta emissions (maximum energy 2.2 MeV) capable of delivering homogeneous radiation to heterogeneous tumors (range 8–100 mm for soft tissue-solid tumors, respectively); and its decay to a stable daughter with no additional toxicities.

Received Apr. 18, 1996; revision accepted Aug. 8, 1996.
For correspondence or reprints contact: Qansy Salako, PhD, Molecular Cancer Institute, 1508 Alhmabra Blvd., Sacramento, CA 95816.

The Nuclear Regulatory Commission and agreement state agencies require that radiopharmaceutical injectables be calibrated to within ±10% of the prescribed dosage (*6,7*). The Capintec radionuclide dose calibrators (Pittsburgh, PA) that have been designed for gamma-emitting radionuclides have become recognized as providing a handy tool for measuring ^{90}Y radiopharmaceuticals using the readily-produced bremsstrahlung radiation. Consequently, it is common for most clinics and other laboratory users to hold the calibration specifications of ^{90}Y suppliers as a reference and relate their own measurements accordingly. Apart from the popular calibrator dial setting of 775 with multiplication factor of 100 (or 775 × 100 dial setting), many laboratories have found that calibrator dial setting of 48 multiplied by 10 will give the suppliers' calibrated activities and hence calibrate their final ^{90}Y drug products. However, some laboratories still use other settings. This prompted Coursey et al. (*7*) of the National Institute of Standards and Technology (NIST) to advise that ^{90}Y users standardize their ^{90}Y sources by liquid scintillation counting (LSC), then use the standard source to establish appropriate dial-factor settings for ^{90}Y dose calibration on their radionuclide dose calibrators.

To investigate variation in calibration of shipments of ^{90}Y from many suppliers, we used LSC to standardize a ^{90}Y test sample and establish the agreement of dose calibrator measurements at dial settings 48 × 10 and 775 multiplied by an appropriate factor. The multiplication factor at which measurements at dial 775 were in agreement was found to be 70 not 100. The effects of quantity of ^{90}Y radioactivity, volume of samples and type of containers were investigated on measurements at these dial settings.

MATERIALS AND METHODS

The ^{90}Y source was purchased from four manufacturers as a carrier-free $^{90}YCl_3$ solution in 0.05 *M* HCl. The source vial from all suppliers was glass (≤1 ml in capacity). One of the sources was standardized by LSC using a Tri-Carb 1500 liquid scintillation analyzer, while all the sources were assayed on a Capintec CRC-12 radionuclide dose calibrator. The plastic Eppendorf tube (1.5 ml), syringes (1 ml and 50 ml) and glass vial (30 ml) used in the calibrator response experiments were purchased from Biorad (Hercules, CA), Becton Dickinson (Rutherford, NJ) and Gensia (Irvine, CA), respectively.